

Final Gleason Score Prediction Using Discriminant Analysis and Support Vector Machine Based on Preoperative Multiparametric MR Imaging of Prostate Cancer at 3T

Fusun Citak Er¹, Metin Vural², Omer Acar³, Tarik Esen⁴, Aslihan Onay², and Esin Ozturk-Isik⁵

¹Genetics and Bioengineering, Yeditepe University, Istanbul, Turkey, ²Department of Radiology, VKF American Hospital, Istanbul, Turkey, ³Department of Urology, VKF American Hospital, Istanbul, Turkey, ⁴School of Medicine, Koc University, Istanbul, Turkey, ⁵Department of Biomedical Engineering, Yeditepe University, Istanbul, Turkey

Introduction: A digital rectal exam (DRE), prostate specific antigen (PSA) level measurement, and transectal ultrasonography guided prostate biopsy (TRUS-Bx) are commonly performed for men with suspected prostate cancer. Additionally, multiparametric MR imaging has been successfully used in detecting, characterizing, and staging the extent of prostate cancer. Treatment planning for prostate cancer is highly patient dependent, and radical prostatectomy is one of the treatment options, which provides a final Gleason score. For patients who don't receive radical prostatectomy, predicting the final Gleason score based on preoperative clinical and MR findings has been an ongoing interest. In this study, we compared predictive performances of linear discriminant analysis (LDA), quadratic discriminant analysis (QDA), support vector machine with linear kernel (SVM-L) and support vector machine with non-linear kernel (SVM-NL) classification algorithms for final Gleason score prediction preoperatively.

Methods: Twenty-six prostate cancer patients (mean age=61.36±6.55) who subsequently underwent radical prostatectomy were included in this study. All subjects provided informed consent. Routine clinical examination included digital rectal examination (DRE) to detect the presence of a palpable prostate abnormality and serum PSA level measurement. Index lesion size was calculated during TRUS-Bx exam. A Gleason score was determined for the pathologic analysis of both the TRUS-Bx sample and radical prostatectomy specimen. All patients were scanned on a 3T MRI scanner (Siemens Healthcare, Erlangen, Germany) using an external phased array body and spine coil. Multiparametric MR imaging protocol included high resolution T2-weighted MR imaging (T2w MRI) in three orthogonal directions (TR/TE=4830/114 ms, number of signal averages (NSA)=2, field of view (FOV)=200 mm, and matrix size 307x512), diffusion-weighted MR imaging (DWI) (TR/TE=4000/78 ms, NSA=6, matrix size=106x128, FOV=260 mm, b=0, 100, 400, 800 s/mm²), and dynamic contrast-enhanced MR imaging (DCE MRI) (TR/TE=5.08/1.74 ms, flip angle=15°, FOV=260 mm, matrix size=138x192, NSA=1). An experienced radiologist determined the Likert scale for each MR imaging modality ranging from one to five. ADC values were calculated. The age of the patient, the presence or absence of a palpable prostate abnormality from rectal examination findings, PSA level, Gleason score based on the pathologic analysis of the TRUS-Bx sample, index lesion size, ADC value, Likert scales of T2w MRI, DW MRI, and DCE MRI were used as the predictors. Linear discriminant analysis (LDA), quadratic discriminant analysis (QDA), support vector machine with linear kernel (SVM-L) and support vector machine with non-linear kernel (SVM-NL) classification algorithms were implemented in MATLAB (Mathworks Inc., Natick, MA). The performance of these classification algorithms for predicting the final Gleason score based on radical prostatectomy specimen based on these nine predictors was assessed. Gleason scores six and seven were specified as low-grade(L), while Gleason score eight and nine were specified as high-grade (H). Nine dimensional data of patients was normalized using unit-variance scaling and mean centering, and the dimension was reduced to five using principal component analysis (PCA). Then, the data was partitioned into test and training datasets using three-fold cross validation. The classification algorithms were trained and tested fifteen times using cross-validation. Finally, the mean sensitivities and specificities of those fifteen epochs were calculated as the final performance measure of the corresponding classifier.

Results and Discussion: Figure 1 shows the washout map (a) and the time curve of a voxel (b) of DCE MRI, an MR spectrum of a tumor voxel displaying high choline and low citrate (c), T2w MRI (d), ADC (e), and T1w MRI (f) of a 67 years old patient diagnosed with prostate cancer. Table 1 shows the mean values of the predictors for low grade and high grade. The age of the patients, DRE findings, index lesion size, and Likert scale of DW MRI were similar in these two groups. High grade group had a higher PSA level, biopsy Gleason score, and Likert scale for T2w MRI and DCE MRI, and a lower ADC than the low grade group. The sensitivities of LDA, QDA, SVM-L, and SVM-NL were 89.69%, 78.37%, 89.05%, and 81.17%, respectively. The specificities of LDA, QDA, SVM-L, and SVM-NL were 60.11%, 55.18%, 70.76%, and 61.07%, respectively. All four classification methods resulted in accurate prediction of final Gleason score based on clinical findings and preoperative multiparametric MR imaging for this limited sample population. Linear discriminant analysis and SVM-L classification resulted in a slightly higher sensitivity than the other methods. Future studies will investigate the role of preoperative MR imaging parameters in Gleason score prediction in a larger patient population.

Table 1. Mean and standart deviations of predictors of the original datasets grouped by Gleason score level.

Predictors	Low Grade (mean±std)	High Grade (mean±std)
Age	60.40±6.31	64.33±5.85
DRE	0.30±0.47	0.33±0.51
PSA	9.05±12.89	12.23±13.77
Biopsy Gleason score	6.65±0.58	8.00±0.89
Index lesion size	1.44±0.34	1.58±0.65
ADC	689.95±148.10	595.50±152.46
Likert scale of T2w MRI	4.05±0.68	4.33±0.52
Likert scale of DW MRI	4.60±0.59	4.66±0.52
Likert scale of DCE MRI	3.95±1.35	5.00±0.00

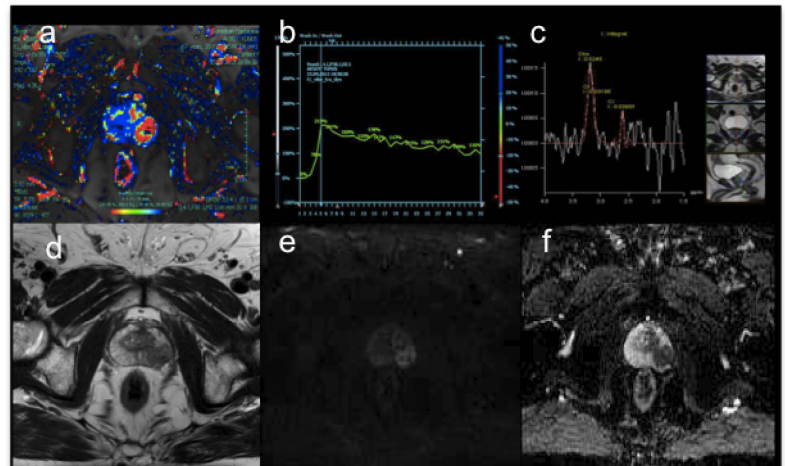


Figure 1. Multiparametric MRI data of a 67 years old male patient diagnosed with prostate cancer. DCE MRI washout map (a), DCE MRI time curve (b), MRS (c), T2w MRI (d), ADC (e), and T1w MRI (f).

References: This study was supported by TUBITAK Career Development Grant 112E036. 1) Jackson, D. and R.D. Riley. "A Refined Method for Multivariate Meta-Analysis and Meta-Regression." *Stat Med* (2013). 2) Mowatt, G., G. Scotland, C. Boachie, M. Cruickshank, J. A. Ford, C. Fraser, L. Kurban, *et al.* "The Diagnostic Accuracy and Cost-Effectiveness of Magnetic Resonance Spectroscopy and Enhanced Magnetic Resonance Imaging Techniques in Aiding the Localisation of Prostate Abnormalities for Biopsy: A Systematic Review and Economic Evaluation." *Health Technol Assess* 17, no. 20 (May 2013): vii-xix, 1-281. 3) R. Likert. "A Technique for the Measurement of Attitudes." *Arch Psychol*, no. 140 (1932): 1-55. 4) Simmons, M. N., R. K. Berglund, and J. S. Jones. "A Practical Guide to Prostate Cancer Diagnosis and Management." *Cleve Clin J Med* 78, no. 5 (May 2011): 321-31.